nature chemistry

ARTICLES

PUBLISHED ONLINE: 22 APRIL 2012 | DOI: 10.1038/NCHEM.1331

Biomimetic radical polymerization via cooperative assembly of segregating templates

Ronan McHale[1], Joseph P. Patterson[1], Per B. Zetterlund[2] and Rachel K. O'Reilly[1]*

Segregation and templating approaches have been honed by billions of years of evolution to direct many complex biological processes. Nature uses segregation to improve biochemical control by organizing reactants into defined, well-regulated environments, and the transfer of genetic information is a primary function of templating. The ribosome, wherein messenger RNA is translated into polypeptides, combines both techniques to allow for ideal biopolymer syntheses. Herein is presented a biomimetic segregation/templating approach to synthetic radical polymerization. Polymerization of a nucleobase-containing vinyl monomer in the presence of a complementary block copolymer template of low molecular weight yields high molecular weight (M_w up to ~400,000 g mol^{-1}), extremely low polydispersity (≤1.08) daughter polymers. Control is attained by segregation of propagating radicals in discrete micelle cores (via cooperative assembly of dynamic template polymers). Significantly reduced bimolecular termination, combined with controlled propagation along a defined number of templates, ensures unprecedented control to afford well-defined high molecular weight polymers.

Segregation is a common strategy in eukaryotic biology wherein individual components are isolated in distinct compartments, for example nuclei or mitochondria. It is used to control various chemical reactions and equilibria within the cell; activation energies can be reduced and reaction rates increased through confinement of reactants in high effective concentrations. Conversely, undesirable interactions can also be avoided through isolation of individual reactants in separate environments. Segregation is also often used in synthetic (non-biological) settings[1–4]. A well-studied example is emulsion polymerization, in which polymerization occurs in monomer-swollen polymer particles dispersed in a continuous aqueous phase. Provided that the particles are sufficiently small (submicron), numerous advantages are reported relative to bulk/solution polymerization, including increased polymerization rate and higher molecular weight (MW). Such phenomena are well-understood and attributed to reduced bimolecular termination between segregated propagating radicals. More recently, it was also demonstrated that segregation effects can lead to improved control over MW distribution and end-group fidelity in controlled/living radical polymerization (CLRP) techniques such as nitroxide-mediated polymerization[4–6] and atom transfer radical polymerization (ATRP)[4,7,8].

Templated synthesis represents another common approach in nature, a primary example being the transcription of nuclear DNA into messenger RNA, followed by translation into peptides and proteins using the machinery of the ribosome. Biological templating mechanisms have evolved to incredible levels of accuracy, with exact control attained over regiochemistry (sequence), stereochemistry (tacticity) and MW (degree of polymerization (DP)). Given these evident advantages, it is unsurprising that the pursuit of polymers capable of templating has also received much attention in synthetic polymer chemistry[9,10], with numerous examples of nucleobase-containing polymers reported[11–23]. Limited progress, however, has been demonstrated in the use of such polymers as templates for the replication of well-defined daughter polymers in a controlled manner[9–12].

Although the recent templated Sonogashira coupling of adenine-containing monomers in the presence of a thymine-containing block copolymer[24] offers undoubted hope for template polymerizations that involve step-growth mechanisms (or less-active propagating species), it is apparent that highly active chain-growth mechanisms, for example radical polymerization, are not easily applied to controlled templating. A probable cause of the lack of success to date is the homogeneous (solution based) nature of the templating approaches investigated thus far[9–12], wherein template polymers exist as discrete random coils in solution. Minimal constraints and a lack of segregation in such systems do little to prevent the interactions of highly reactive propagating radicals with other propagating species and/or monomers on neighbouring template(s). As such, propagation events almost certainly occur across an arbitrary number of template species, with little control over termination leading to ill-defined polymer products.

Biology uses segregation concurrently with templating to perform precise syntheses and manipulations in a regulated environment. Here we describe a bioinspired dual segregation/templating approach to radical polymerization, wherein a synthetic nucleic acid analogue (poly(styrene-*b*-vinylbenzyl thymine) (PSt-*b*-PVBT)) is used to both template and segregate complementary poly(vinylbenzyl adenine) (PVBA) chains as they propagate. Radical polymerization in such an environment affords a significant benefit over traditional solution-based templating approaches, chiefly the elimination or vast reduction of bimolecular termination. When combined with controlled propagation along a defined number of templates, a free radical (non-CLRP) route to very low polydispersity index (PDI) (≤1.08) and high MW (up to ~400,000 g mol^{-1}) polymers is realized. We propose that this combined segregation/templating approach represents a significant step towards fundamental goals in the field of polymer science, such as sequence-controlled polymerization[25–29] and controlled polymer folding[30–35].

Results and discussion

Template synthesis and assembly. Vinylbenzyl thymine (VBT) and vinylbenzyl adenine (VBA) monomers were prepared from vinylbenzyl chloride and the corresponding nucleobases, as

[1]Department of Chemistry, Library Road, University of Warwick, Coventry, CV4 7AL, UK, [2]Centre for Advanced Macromolecular Design (CAMD), School of Chemical Engineering, University of New South Wales, Sydney, NSW 2052, Australia. *e-mail: Rachel.OReilly@warwick.ac.uk

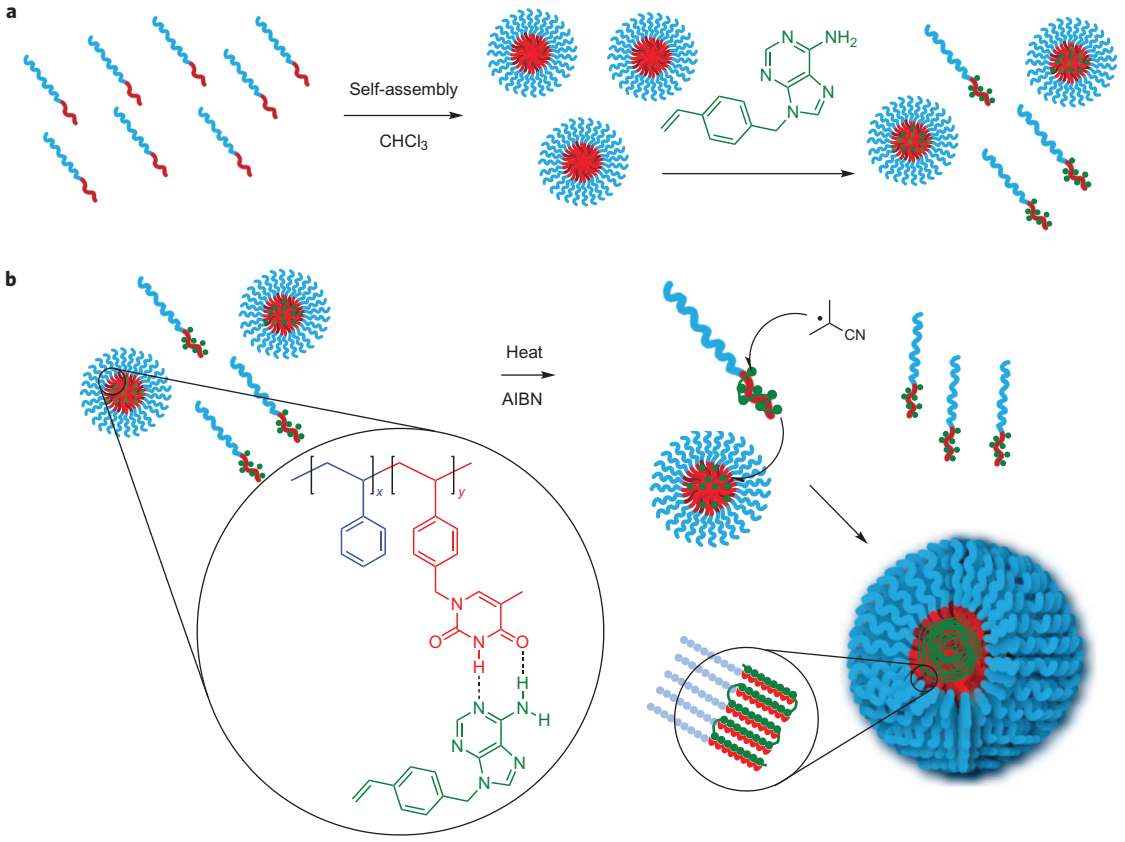

Figure 1 | Dynamic exchange and cooperative assembly of templates. a, Self-assembly of template block copolymer PSt-*b*-PVBT in $CHCl_3$ yields a stable monodisperse micellar system with PVBT cores. The addition of a complementary adenine monomer (VBA) induces dynamic exchange of VBA-loaded template unimers. **b**, On the addition of AIBN and heating, it is proposed that VBA initiation occurs on an exchanging unimer before returning to a micelle for continued propagation. Further dynamic VBA-loaded unimers add to the initiated micelle, from a reservoir of non-initiated micelles, to yield a stable, non-dynamic larger micelle that contains the high MW, low PDI PVBA daughter polymer.

described elsewhere[36] (see Supplementary Fig. S1a for ^{1}H NMR spectra). A PSt_{115}-*b*-$PVBT_{18}$ block copolymer template was prepared using nitroxide ((2,2,6,6-tetramethylpiperidin-1-yl)oxyl (TEMPO))-mediated polymerization in dimethylformamide (DMF) at 125 °C (see Supplementary Information and Supplementary Fig. S1b). TEMPO-mediated synthesis was preferred over other CLRP techniques to ensure a chemically inert template at 60 °C, given that the rate of activation of TEMPO-terminated polystyrene (PSt-TEMPO) is negligible at this temperature[37,38]. Furthermore, in the design of the template a PSt block was employed to enhance template solubility in a relatively non-polar solvent, for example chloroform ($CHCl_3$). Such a solvent is crucial in promoting stronger H-bonding between complementary nucleobases (that is, negligible solvent–nucleobase interactions). A pyrimidine nucleobase (thymine) was selected as the basis of the polymeric template in this study as there is evidence to suggest that intramolecular H-bonding in alternative purine-containing species adversely affects their ability to perform as templates[12].

PSt_{115}-*b*-$PVBT_{18}$ block copolymers self-assembled into micelles on direct dissolution in $CHCl_3$ at room temperature at 10 mg ml^{-1} (Fig. 1). Dynamic light-scattering (DLS) analysis revealed structures of narrow size distribution with an intensity average diameter (I_{av}) of ~26 nm and a PD of ~0.1 (see Supplementary Fig. S2a). Micelle size and distribution showed nominal concentration and temperature dependence, which indicates a stable assembly. Static light-scattering (SLS) analysis (Zimm plot, Supplementary Fig. S2b) determined the micellar weight-average molecular weight (M_w) to be 476,000 g mol^{-1}, which corresponds to an aggregation number of ~24 (taking M_w of PSt_{115}-*b*-$PVBT_{18}$ as 19,800 g mol^{-1}; see Supplementary Information). Zimm analysis is appropriate in the current system because of the narrow size distribution and relative independence of micelle diameter (I_{av}) on concentration. A representative transmission electron microscopy (TEM) image of PSt_{115}-*b*-$PVBT_{18}$ in $CHCl_3$ is shown in Fig. 2a, and illustrates the formation of uniform, spherical micelles (average diameter by TEM, ~13 nm). ^{1}H NMR spectroscopy in $CDCl_3$ confirmed PSt as the coronal block with PVBT confined to a relatively immobile core domain at room temperature. Core mobility was, however, observed on heating to 60 °C (Supplementary Fig. S2c).

Addition of complementary monomer. VBA is only partially soluble in $CHCl_3$ at room temperature. However, in the presence of PSt_{115}-*b*-$PVBT_{18}$, VBA solutions in $CHCl_3$ became homogeneous on stirring, which provided preliminary evidence for a complementary interaction between VBA and the block copolymer template. More definitive evidence for adenine–thymine base pairing was obtained from ^{1}H NMR spectroscopy, wherein pronounced PVBT core block resonances appeared on the addition of VBA to micellar solutions of the template in $CDCl_3$ (Supplementary Fig. S3a). Specifically, the downfield resonance at 11–12 ppm, corresponding to the H-bonded NH of VBT[17], and another at ~4.7 ppm (corresponding to CH_2N) appeared on the addition of VBA at room temperature. This suggests considerable mobility in the micelle core and dynamic exchange in the presence of the complementary monomer, similar to that reported by Epps and co-workers on the addition of

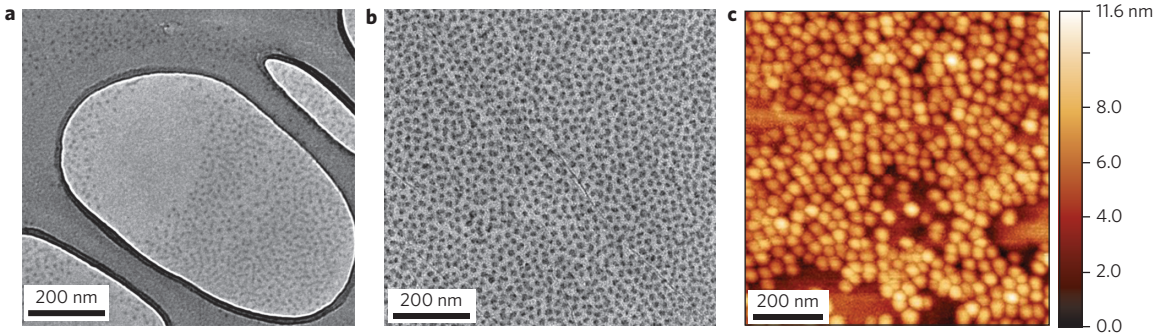

Figure 2 | Microscopic characterization of micellar assemblies. a, TEM image of PSt_{115}-*b*-$PVBT_{18}$ micelles prior to VBA addition. **b**, TEM image of micelles obtained after the addition and polymerization of VBA in the presence of PSt_{115}-*b*-$PVBT_{18}$. **c**, AFM height image of the micelles in (**b**). TEM and AFM analyses were conducted on a sample drop deposited on a lacey carbon grid coated with an atomically thin layer of graphene oxide (GO)[40]. The lighter region in (**a**) is the GO coating over a hole in the lacey carbon support (darker/thicker region). The observed contrast in the TEM images was achieved without staining (see Supplementary Information for further details).

increasing levels of tetrahydrofuran (THF) to micellar systems[39]. Further evidence for such dynamic behaviour was obtained from a light-scattering comparison of the micellar assembly before and after the addition of VBA. A significant decrease in scattered light intensity was observed over a range of temperatures on the addition of VBA (Supplementary Fig. S3b), with little change observed in the overall diameter (Supplementary Fig. S3c).

Template polymerization via cooperative assembly. VBA polymerizations in the presence of PSt-*b*-PVBT were initiated using 2,2′-azobisisobutyronitrile (AIBN) as the free-radical source (~10% excess VBA added relative to VBT units in the template; see Supplementary Information for details). A representative size-exclusion chromatography (SEC) trace (conducted in dimethylacetamide (DMAc) solvent) of the polymer mixture obtained at 28% VBA conversion, in the presence of PSt_{107}-*b*-$PVBT_{24}$, is shown in Fig. 3 (initiation at 60 °C for one hour followed by cooling to 45 °C for a further two hours; see Supplementary Fig. S4a–c and associated discussion for optimization of the polymerization temperature). A high MW, extremely low PDI peak (retention time ≈ 12 minutes, $M_n \approx 262{,}500\ g\ mol^{-1}$, PDI = 1.05, relative to poly(methyl methacrylate) (PMMA) standards) was observed, distinct from the original template block copolymer peak (retention time ≈ 14.5 minutes). Importantly, neither the retention time nor the distribution of the block copolymer template peak changed significantly during the polymerization of VBA, as expected given the inactivity of PSt-TEMPO at temperatures ≤60 °C (refs 37,38). Further SEC experiments were performed on mixtures of low MW PVBA materials to rule out the formation of high MW polymer aggregates rather than single PVBA chains (see Supplementary Fig. S8f).

DLS analysis of the assemblies after polymerization of VBA in the presence of PSt_{115}-*b*-$PVBT_{18}$ revealed an increase in micelle diameter from ~26 nm (I_{av}) to ~34 nm (I_{av}) on the addition and polymerization of VBA (Supplementary Fig. S5a). Further to the size increase, a narrowing of the PD from ~0.13 (dynamic system in the presence of VBA, Supplementary Fig. S3c) to ~0.05 (after polymerization of VBA, Supplementary Fig. S4a) was also observed. TEM and atomic force microscopy (AFM) images of the micelles formed after the addition and polymerization of VBA are shown in Fig. 2b,c. In agreement with the DLS data, it is apparent from TEM that the micelles increased significantly in size from ~13 nm to ~20 nm and retained a narrow size distribution (see Supplementary Figs S5b (TEM) and S5c (AFM) for additional images).

An analogous polymerization conducted in $CDCl_3$ (to facilitate direct ^{1}H NMR spectroscopy of the crude polymerization mixture) revealed an absence of VBT core block signals after polymerization; that is, a return to the non-dynamic system observed prior to the addition of VBA. Crucially, a large decrease in VBA monomer signals (both vinyl and otherwise) was also observed, which indicates confinement of PVBA to a segregated, non-dynamic core on polymerization (Supplementary Fig. S5d).

High MW daughter polymer was isolated from low MW template polymer by small-scale preparative SEC in DMAc (see Supplementary Information for details). A ^{1}H NMR spectrum of the isolated polymer confirmed the newly generated daughter polymer as a PVBA homopolymer (see Supplementary Fig. S6), with the corresponding SEC traces before and after separation shown in Fig. 3. The retention time (and associated M_n) and distribution of the peak remained unchanged in the absence of the template, with an extremely low PDI retained.

Control experiments. To discount definitively any TEMPO involvement in the template-mediated radical polymerization, an analogous block copolymer template was synthesized via another CLRP protocol (reversible addition fragmentation chain transfer (RAFT); PSt_{81}-*b*-$PVBT_{19}$, PDI = 1.13; see Supplementary Information for details). Unlike the TEMPO-mediated synthesis, rigorous trithiocarbonate (end group) removal was necessary to ensure the RAFT block copolymer operated only as a template and not as a chain-transfer agent. The removal process was repeated three times with rigorous purification at each stage to ensure quantitative end-group elimination (Supplementary Fig. S7a). The resultant template (PSt_{81}-*b*-$PVBT_{19}$) behaved in a similar fashion to the TEMPO-mediated templates, assembling in $CHCl_3$ to yield well-defined micelles ($I_{av} \approx 22$ nm, PD < 0.1; see Supplementary Fig. S7b for TEM and DLS data). On polymerization of VBA in the presence of the RAFT-synthesized template, micelle size increased to ~28 nm and the PD remained <0.1. A high MW daughter polymer peak was again observed ($M_n \approx 153{,}000\ g\ mol^{-1}$, PDI = 1.14; Supplementary Fig. S7c), which provides strong evidence to rule out any involvement of TEMPO in controlling the templated polymerization.

Further control experiments confirmed the necessity for a specific templating interaction in the present synthesis. First, VBT monomer was polymerized in the presence of PSt_{115}-*b*-$PVBT_{18}$, with no high MW polymer observed. Instead, a very slight broadening of the template SEC trace at low MW (Supplementary Fig. S8a) suggested some off-template polymerization. Ill-defined, low MW polymer (Supplementary Fig. S8b) was obtained on polymerization of VBA in the absence of template in $CHCl_3$ at 60 °C. Preliminary investigations were also conducted on an adenine analogue of PSt-*b*-PVBT, namely PSt_{113}-*b*-$PVBA_{18}$ (PDI = 1.26, TEMPO-mediated;

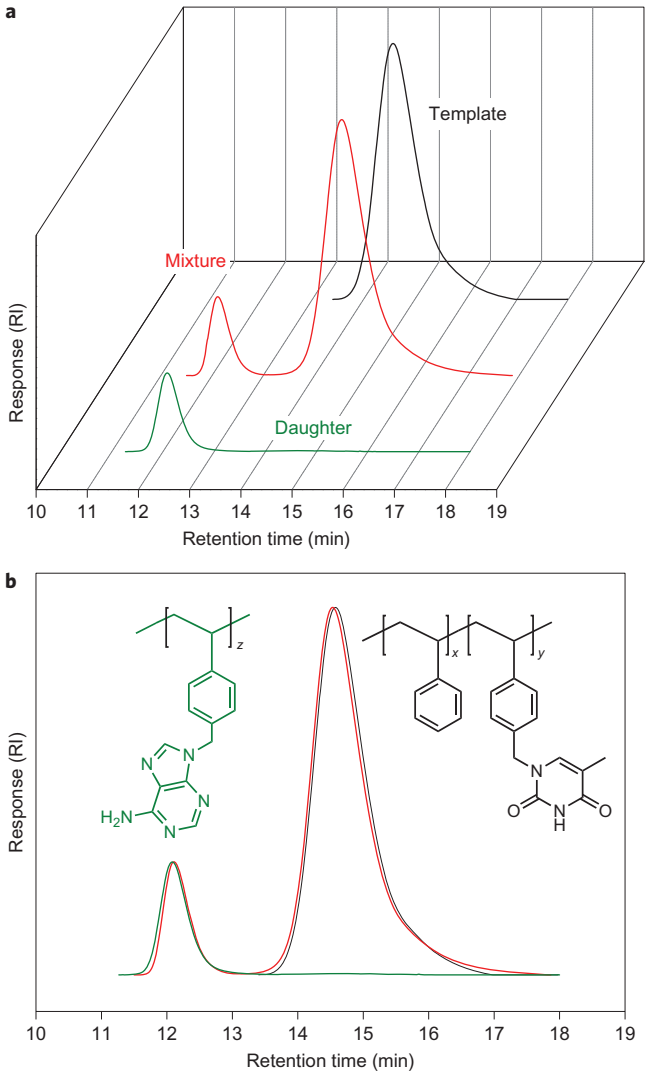

Figure 3 | High MW daughter polymer and template. a, SEC traces (DMAc) of PSt-*b*-PVBT template (black), the mixture of daughter (small peak) and template (large peak) polymers obtained after the polymerization of VBA in the presence of PSt-*b*-PVBT (red; M_n of the high MW daughter polymer peak of ~262,500 g mol^{-1} relative to PMMA standards, PDI = 1.05) and after purification to remove the template polymer (green; $M_n \approx$ 266,200 g mol^{-1}, PDI = 1.07). The PSt-*b*-PVBT micelles dissociate to release PVBA into solution on the removal of $CHCl_3$ and dissolution in DMAc prior to SEC analysis. **b**, A two-dimensional representation of (**a**) to illustrate the precise overlap of (1) the template traces before and after VBA polymerization and (2) the daughter polymer traces before and after separation. See Supplementary Fig. S6 for a ^{1}H NMR spectrum that confirms the high MW peak as the PVBA homopolymer. The separation shown was conducted after the polymerization of VBA in the presence of PSt_{107}-*b*-$PVBT_{24}$ to 28% conversion (one hour at 60 °C and two hours at 45 °C; see Supplementary Table S1b).

Supplementary Fig. S8c). Polymerization of VBT in the presence of PSt_{113}-*b*-$PVBA_{18}$ yielded some high MW products, but the MW distribution was ill-defined (Supplementary Fig. S8d). This result is in keeping with the previous assertion[12] that poly(adenine) species are not favoured for templated synthesis because of adenine–adenine interactions, which inhibit template-monomer recognition. Interestingly, polymerization of VBA in the presence of PSt_{113}-*b*-$PVBA_{18}$ yielded some (albeit minimal) monomodal high MW polymer (Supplementary Fig. S8e), which suggests adenine–adenine interactions may be sufficient for successful templated syntheses using this protocol. Further investigations are currently underway into these and similar systems.

Polymerization mechanism. Previously, a so-called 'hopping' mechanism was proposed to rationalize the generation of high MW daughter polymers in template polymerizations conducted in homogeneous (non-micellar) systems[41–43]. It is apparent that propagation events occur between propagating radicals on one template and monomer units on adjacent templates, the net effect being the generation of high MW daughter polymers (multiple times the MW of single templates). Crucially, 'hopping' across an arbitrary number of templates in previous systems led to a lack of control over MW and PDI. In the current system, however, it is evident that 'hopping' across a defined number of templates (as present in the segregated micelle core) yields unprecedented control over radical polymerization.

A distinct change from a dynamic micellar system (Supplementary Figs S2c and S3a) to a non-dynamic micellar system (Supplementary Fig. S5d) occurs on the addition and polymerization of VBA. It is proposed that polymerization of an individual PVBA chain initiates on an exchanging VBA-loaded PSt-*b*-PVBT unimer before entering a VBA-loaded micelle (Fig. 1). Propagation continues within the micelle by 'hopping' onto other VBA-containing templates in the core. The site of initiation is crucial; it is unlikely that AIBN will initiate in the confined space of the original micelles because of the high probability of geminate coupling of AIBN-derived radical pairs. Significant dynamic exchange of VBA-loaded unimers between micelles makes it more probable that initiation occurs on these unimers, followed by micellar entry.

Polymerization of a single chain in an individual micelle is expected to be fast because of the combined effects of a high effective monomer concentration and alignment of VBA monomer along templates in the core. As such, full growth of individual chains is attained prior to interaction with other radicals that may enter the same micelle. Evidence for fast propagation is obtained from the production of high MW daughter polymers at low conversions; that is, this is not a living polymerization (M_n is independent of conversion at constant temperature; see Fig. 4 and Supplementary Figs S4a–c).

Micellar growth and/or rearrangement. Zimm analysis was conducted postpolymerization to assess the M_w of the micelles after daughter polymer formation. The most striking finding from this analysis was a significant (about fourfold) increase in micellar M_w from 476,000 to 1,894,000 g mol^{-1} on the addition and polymerization of VBA (Supplementary Fig. S5e). Such an increase is indicative of micellar growth and/or rearrangement on the polymerization of VBA. As 30 wt% VBA monomer was added relative to the template block copolymers that comprised the original micelles, the maximum permissible increase in micellar M_w in the event of simple swelling and polymerization of VBA in the core of the original micelles, without rearrangement, is 30%. In the unlikely event of ideal 1:1 VBA–VBT templating, a pre-VBA micellar M_w of 476,000 g mol^{-1} (containing ~27 wt% VBT) would be expected to template a PVBA daughter polymer of maximum $M_w \approx$ 130,000 g mol^{-1} at 100% monomer conversion, with an associated micellar M_w increase to just ~600,000 g mol^{-1}. This further supports micellar rearrangement, given the much higher MW of the daughter polymer (~300,000 g mol^{-1}) and final micellar MW.

Dynamic exchange. The observed dynamic micellar behaviour is deemed crucial in rationalizing the fourfold increase in micellar M_w. It is proposed that the addition of dynamic VBA-loaded

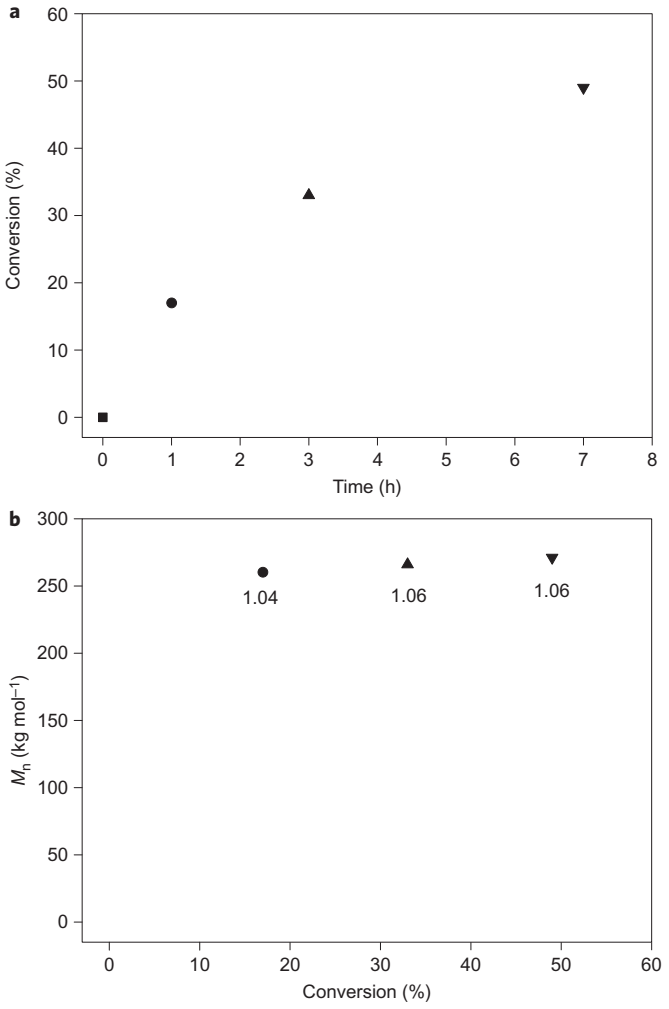

Figure 4 | Polymerization rate and MW versus conversion. a, Typical conversion–time data. **b**, Daughter polymer M_n (and PDI values) versus conversion at constant temperature (60 °C), illustrating the generation of the high MW daughter polymer at low conversion and the subsequent independence of M_n and conversion (see Supplementary Fig. S4b and associated discussion for further details).

unimers increases micellar M_w significantly. Those unimers that enter an 'initiated micelle', that is a micelle wherein VBA polymerization has been initiated, should have restricted mobility on the polymerization of their VBA cargo because of significant PVBA–PVBT interactions. As such, 'non-initiated micelles' are expected to act as a reservoir of VBA-loaded unimers that feed into the initiated micelles. Hawkett and co-workers described a similar mechanism for particle growth in RAFT-mediated emulsion polymerization in which some micelles are initiated and others serve as a diblock reservoir to grow those that are initiated[44].

Assembly of the final micelle is expected to continue until further unimers are prevented from entering the core. Given the remarkable control observed, it is evident that micellar reorganization occurs on a timescale sufficiently rapid to ensure negligible side reactions; that is, propagating chains become segregated into a micellar assembly prior to bimolecular termination or further significant initiation events. Supporting evidence for the fast segregation of propagating radicals can be derived from the observation that M_n and PDI are independent of AIBN concentration (within the range studied; see Supplementary Fig. S9a).

Postpolymerization Zimm analysis ($M_w \approx 1{,}894{,}000$ g mol^{-1}) suggests a final micelle that contains approximately one daughter polymer chain per micelle and, based on this analysis, the aggregation number of PSt_{115}-*b*-$PVBT_{18}$ chains necessary to template a daughter polymer of $M_w \approx 300{,}000$ g mol^{-1} could be determined. Although it is possible that some of the new micelles contain two or more daughter polymer chains after template polymerization, the low PDI (1.05) observed in the final daughter polymer also suggests an average of one daughter chain per micelle.

Effect of template MW. A larger MW template (PSt_{232}-*b*-$PVBT_{39}$) also produces a high MW, extremely low PDI daughter polymer (386,000 g mol^{-1}, PDI = 1.05). Although Zimm analysis prior to the addition of VBA (micellar $M_w \approx 3{,}924{,}000$ g mol^{-1}) and postpolymerization (micellar $M_w \approx 5{,}220{,}000$ g mol^{-1}) suggests a smaller degree of rearrangement in the case of the higher MW template polymer, the high MW and extremely low PDI daughter polymer indicate a similar mechanism. Data obtained using this significantly larger diblock copolymer template is included in Supplementary Fig. S10a,b. Possible reasons for a reduced rearrangement in the higher MW template system include: (1) smaller micellar surface area in the larger micelles, (2) less capacity to accept unimers in the already high M_w micelles and (3) possible reduced dynamic behaviour of the larger template unimers. Additional supporting mechanistic data are discussed further in the Supplementary Information, including the observation that the M_n of the daughter polymer is not markedly altered on reducing the VBA concentration (see Fig. S9b and associated discussion therein).

Radical polymerization in a segregated environment. Notable examples of radical polymerization in segregated environments include the polymerization of styrene and other monomers in metal–organic framework (MOF) nanochannels[45] and the polymerization of methacrylates through stereocomplex formation within a stereoregular film[46]. Although increased radical lifetimes were postulated in both systems, MWs were significantly lower and PDI values significantly higher than those observed in the current system ($M_n = 11{,}100$ g mol^{-1} and PDI = 1.50 in the MOF nanochannels[45] and $M_n = 39{,}300$ g mol^{-1} and PDI = 1.90 in the stereoregular polymerization)[46]. Another elegant example of radical polymerization in a segregated environment is the so-called 'self-encapsulating' radical polymerization described by Percec *et al.*[47,48]. Polymerization-induced assembly of mono dendritic monomers yielded spherical or cylindrical polymers, depending on the DP. Akin to the current synthesis, encapsulation of propagating radicals yielded good control over polymerization kinetics, with PDI values less than 1.10. However, such control was only feasible at very low degrees of polymerization (DP ≈ 5, $M_n \approx 12{,}000$ g mol^{-1}, spherical assembly of dendrimers). At higher degrees of polymerization, cylindrical polymers were formed that had significantly larger PDI values (≥2.36).

High MW, low PDI (<1.10) materials prepared by radical polymerization have proved elusive and are currently only attainable using stringent CLRP conditions. One such approach, demonstrated using RAFT[49], employs high-pressure polymerization to increase the propagation rate relative to that of termination, which results in a well-defined high MW PMMA (MW > 10^6 g mol^{-1}, PDI = 1.03). Metal-catalysed approaches, such as single-electron transfer living radical polymerization[50], reverse ATRP in mini-emulsion[7,8] and activators regenerated by electron transfer ATRP[51], have given similar high MWs at ambient pressure, but higher PDI values (~1.20).

Conclusions

Radical polymerization of an adenine-containing vinyl monomer in the presence of a complementary thymine-containing block

copolymer template yields a high MW (M_w up to ~400,000 g mol^{-1}), extremely low PDI (≤1.08) daughter polymer via segregation of propagating chains in discrete micelle cores. To the best of our knowledge, the current contribution is the first example of such well-defined polymers from a conventional (non-CLRP) radical polymerization mechanism. A more significant impact of this contribution, however, may ultimately be the success demonstrated in chain manipulation during radical propagation.

Current CLRP techniques, although undoubtedly a huge advance in the field, seek largely to maintain distributive control within a population of polymer chains, with minimal control over the primary structure. Manipulation of individual chains, as demonstrated herein with the segregation of chains in micelle cores as they propagate, promises unheralded control over more critical aspects of primary polymer structure, such as tacticity and regiochemistry[52]. If we are to succeed in some of the fundamental long-term goals of our field, such as sequence control and single-chain folding, it is key that further emphasis be focused on such manipulation at the (macro)molecular level.

Methods

Full details of experimental methods (materials, instrumentation, synthesis, etc.) are available in the Supplementary Information.

TEMPO-mediated synthesis of PSt. TEMPO (0.022 g, 1.41 × 10^{-4} mol) and AIBN (0.017 g, 1.04 × 10^{-4} mol) were dissolved in styrene (10.0 g, 9.6 × 10^{-2} mol). After three freeze–thaw degas cycles on a Schlenk apparatus (the same procedure was used for all polymerizations below), the light orange mixture was heated under N_2 at 125 °C for 65 minutes. ^{1}H NMR spectroscopy of the crude mixture in $CDCl_3$ indicated that monomer conversion was ~16%. The resultant polymer was purified by the addition of the crude mixture to MeOH (~250 ml) for precipitation, followed by filtration. The precipitation procedure was repeated twice from concentrated $CHCl_3$ solutions of the polymer, followed by filtration and drying *in vacuo*. The polymer was confirmed as monomer- and solvent-free by ^{1}H NMR spectroscopy in $CDCl_3$. SEC in THF versus PSt standards determined M_n as 12,150 g mol^{-1} (PDI = 1.25, PSt_{115}).

TEMPO-mediated synthesis of PSt-*b*-PVBT. A typical synthesis was as follows: PSt_{115} (TEMPO functionalized) (1.0 g, 8.23 × 10^{-5} mol) and VBT (1.0 g, 4.13 × 10^{-3} mol) were dissolved in DMF (6 ml) before polymerization under N_2 at 125 °C for 20 hours (36% conversion (by ^{1}H NMR spectroscopy)). The polymer was purified by repeated precipitation in MeOH (final two precipitations from $CHCl_3$) and analysed by ^{1}H NMR spectroscopy in d_7-DMF. SEC in DMAc (versus PMMA standards) revealed a narrow monomodal peak (PDI = 1.20). DP of the VBT block was determined from ^{1}H NMR spectroscopy (PSt_{115}-*b*-$PVBT_{18}$, M_n (NMR spectroscopy) ≈ 16,500 g mol^{-1}, M_w ≈ 19,800 g mol^{-1}). Two distinct glass transition temperature (T_g) values of ~105 °C (PSt block) and 186 °C (PVBT block) were observed for PSt_{107}-*b*-$PVBT_{24}$ (by differential scanning calorimetry (DSC)).

Template assembly and characterization. Micelles were prepared by the direct dissolution of PSt-*b*-PVBT in $CHCl_3$ at room temperature and characterized by a variety of techniques, including DLS, SLS, ^{1}H NMR spectroscopy and TEM (see Supplementary Information). TEM analysis was conducted on lacey carbon grids (400 Mesh, Cu, Agar Scientific) coated in a thin layer of graphene oxide (GO)[40]. One drop (*ca.* 0.08 ml) of sonicated GO solution was deposited onto each grid and left to air dry for *ca.* 30 minutes. Once dry, the grids could be stored for several weeks before sample deposition. To deposit micellar assemblies, a small drop (*ca.* 2–10 μl) of sample was pipetted onto a pre-prepared GO grid and left to air dry. All samples were examined with a JEOL TEM-1200 transmission electron microscope, operating at 100 kV without the addition of a staining agent[40].

Polymerization of VBA in the presence of PSt-*b*-PVBT. A typical template polymerization consisted of PSt_{115}-*b*-$PVBT_{18}$ (0.02 g, 1.21 × 10^{-6} mol) and AIBN (0.0003 g, 1.83 × 10^{-6} mol) in $CHCl_3$ (2.0 ml) to which was added VBA (0.006 g, 2.39 × 10^{-5} mol). A ~10% excess of VBA was added relative to the VBT units in the template. Stock solutions were used to ensure accuracy. The $CHCl_3$ solutions were subjected to three freeze–thaw degas cycles before heating under N_2 at the requisite temperature. Polymerizations were typically initiated at 60 °C for one hour and then the temperature reduced to 45 °C for the remainder of the polymerization. DLS analysis was conducted on crude polymerization mixtures after filtration using a 0.2 μm poly(tetrafluoroethylene) filter. $CHCl_3$ was removed *in vacuo* prior to dissolution of a sample in DMAc for SEC analysis and d_6-dimethylsulfoxide for conversion analysis via ^{1}H NMR spectroscopy. VBA polymerizations in the presence of a higher MW template (PSt_{232}-*b*-$PVBT_{39}$) were conducted in a similar manner to the above using the following procedure: PSt_{232}-*b*-$PVBT_{39}$ (0.02 g, 5.90 × 10^{-7} mol) and AIBN (0.0003 g, 1.83 × 10^{-6} mol) were dissolved in $CHCl_3$ (2.0 ml) to which was added VBA (0.006 g, 2.39 × 10^{-5} mol).

Separation of the PVBA daughter polymer from PSt-*b*-PVBT. A 500 μl sample loop was fitted to the PL-SEC-50 described in the Supplementary Information (DMAc solvent, mixed C columns). Concentrated samples (~10 mg ml^{-1}) of the polymer mixture (in DMAc) were injected onto the columns and the high MW PVBA daughter polymer peak was collected. The above injection was repeated at least ten times to collect sufficient PVBA for ^{1}H NMR spectroscopic analysis.

Received 3 October 2011; accepted 13 March 2012; published online 22 April 2012

References

1. Vriezema, D. M. *et al.* Self-assembled nanoreactors. *Chem. Rev.* **105,** 1445–1490 (2005).
2. Monteiro, M. J. Nanoreactors for polymerizations and organic reactions. *Macromolecules* **43,** 1159–1168 (2010).
3. Sebakhy, K. O., Kessel, S. & Monteiro, M. J. Nanoreactors to synthesize well-defined polymer nanoparticles: decoupling particle size from molecular weight. *Macromolecules* **43,** 9598–9600 (2010).
4. Zetterlund, P. B. Controlled/living radical polymerization in nanoreactors: compartmentalization effects. *Polym. Chem.* **2,** 534–549 (2011).
5. Zetterlund, P. B. & Okubo, M. Compartmentalization in nitroxide-mediated radical polymerization in dispersed systems. *Macromolecules* **39,** 8959–8967 (2006).
6. Maehata, H., Buragina, C., Cunningham, M. & Keoshkerian, B. Compartmentalization in TEMPO-mediated styrene miniemulsion polymerization. *Macromolecules* **40,** 7126–7131 (2007).
7. Simms, R. W. & Cunningham, M. F. High molecular weight poly(butyl methacrylate) by reverse atom transfer radical polymerization in miniemulsion initiated by a redox system. *Macromolecules* **40,** 860–866 (2007).
8. Simms, R. W. & Cunningham, M. F. Compartmentalization of reverse atom transfer radical polymerization in miniemulsion. *Macromolecules* **41,** 5148–5155 (2008).
9. Tan, Y. Y. The synthesis of polymers by template polymerization. *Prog. Polym. Sci.* **19,** 561–588 (1994).
10. Polowinski, S. Template polymerization and co-polymerization. *Prog. Polym. Sci.* **27,** 537–577 (2002).
11. Inaki, Y. Synthetic nucleic acid analogs. *Prog. Polym. Sci.* **17,** 515–570 (1992).
12. Khan, A. *et al.* Hydrogen bond template-directed polymerization of protected 5′-acryloylnucleosides. *Macromolecules* **32,** 6560–6564 (1999).
13. Marsh, A., Khan, A., Haddleton, D. M. & Hannon, M. J. Atom transfer polymerization: use of uridine and adenosine derivatized monomers and initiators. *Macromolecules* **32,** 8725–8731 (1999).
14. Marsh, A., Khan, A., Garcia, M. & Haddleton, D. M. Copper(I) mediated radical polymerisation of uridine and adenosine monomers on a silica support. *Chem. Commun.* 2083–2084 (2000).
15. Ilhan, F. *et al.* Giant vesicle formation through self-assembly of complementary random copolymers. *J. Am. Chem. Soc.* **122,** 5895–5896 (2000).
16. Thibault, R. J. *et al.* Specific interactions of complementary mono- and multivalent guests with recognition-induced polymersomes. *J. Am. Chem. Soc.* **124,** 15249–15254 (2002).
17. Lutz, J-F., Thünemann, A. F. & Nehring, R. Preparation by controlled radical polymerization and self-assembly via base-recognition of synthetic polymers bearing complementary nucleobases. *J. Polym. Sci. Part A: Polym. Chem.* **43,** 4805–4818 (2005).
18. Spijker, H. J., Dirks, A. J. & van Hest, J. C. M. Unusual rate enhancement in the thymine assisted ATRP process of adenine monomers. *Polymer* **46,** 8528–8535 (2005).
19. Spijker, H. J., Dirks, A. J. & van Hest, J. C. M. Synthesis and assembly behavior of nucleobase-functionalized block copolymers. *J. Polym. Sci. Part A: Polym. Chem.* **44,** 4242–4250 (2006).
20. Spijker, H. J., van Delft, F. L. & van Hest, J. C. M. Atom transfer radical polymerization of adenine, thymine, cytosine, and guanine nucleobase monomers. *Macromolecules* **40,** 12–18 (2007).
21. Mather, B. D. *et al.* Supramolecular triblock copolymers containing complementary nucleobase molecular recognition. *Macromolecules* **40,** 6834–6845 (2007).
22. Saito, K., Ingalls, L. R., Lee, J. & Warner, J. C. Core-bound polymeric micellar system based on photocrosslinking of thymine. *Chem. Commun.* 2503–2505 (2007).
23. Kaur, G. *et al.* Bioinspired core-crosslinked micelles from thymine-functionalized amphiphilic block copolymers: hydrogen bonding and photo-crosslinking study. *J. Polym. Sci. Part A: Polym. Chem.* **49,** 4121–4128 (2011).
24. Lo, P. K. & Sleiman, H. F. Nucleobase-templated polymerization: copying the chain length and polydispersity of living polymers into conjugated polymers. *J. Am. Chem. Soc.* **131,** 4182–4183 (2009).
25. Ida, S., Terashima, T., Ouchi, M. & Sawamoto, M. Selective radical addition with a designed heterobifunctional halide: a primary study toward sequence-controlled polymerization upon template effect. *J. Am. Chem. Soc.* **131,** 10808–10809 (2009).

26. Ida, S., Ouchi, M. & Sawamoto, M. Template-assisted selective radical addition toward sequence-regulated polymerization: Lariat capture of target monomer by template initiator. *J. Am. Chem. Soc.* **132,** 14748–14750 (2010).
27. Hibi, Y., Ouchi, M. & Sawamoto, M. Sequence-regulated radical polymerization with a metal-templated monomer: repetitive ABA sequence by double cyclopolymerization. *Angew. Chem. Int. Ed.* **50,** 7434–7437 (2011).
28. Hibi, Y. *et al.* Design of AB divinyl 'template monomers' toward alternating sequence control in metal-catalyzed living radical polymerization. *Polym. Chem.* **2,** 341–347 (2011).
29. Ida, S., Ouchi, M. & Sawamoto, M. Designer template initiator for sequence regulated polymerization: systems design for substrate-selective metal-catalyzed radical addition and living radical polymerization. *Macromol. Rapid Commun.* **32,** 209–214 (2011).
30. Harth, E. *et al.* A facile approach to architecturally defined nanoparticles via intramolecular chain collapse. *J. Am. Chem. Soc.* **124,** 8653–8660 (2002).
31. Cherian, A. E., Sun, F. C., Sheiko, S. S. & Coates, G. W. Formation of nanoparticles by intramolecular cross-linking: following the reaction progress of single polymer chains by atomic force microscopy. *J. Am. Chem. Soc.* **129,** 11350–11351 (2007).
32. Foster, E. J., Berda, E. B. & Meijer, E. W. Metastable supramolecular polymer nanoparticles via intramolecular collapse of single polymer chains. *J. Am. Chem. Soc.* **131,** 6964–6966 (2009).
33. Mes, T., van der Weegen, R., Palmans, A. R. A. & Meijer, E. W. Single-chain polymeric nanoparticles by stepwise folding. *Angew. Chem. Int. Ed.* **50,** 5085–5089 (2011).
34. Terashima, T. *et al.* Single-chain folding of polymers for catalytic systems in water. *J. Am. Chem. Soc.* **133,** 4742–4745 (2011).
35. Schmidt, B. V. K. J., Fechler, N., Falkenhagen, J. & Lutz, J-F. Controlled folding of synthetic polymer chains through the formation of positionable covalent bridges. *Nature Chem.* **3,** 234–238 (2011).
36. Yang, X. *et al.* Synthesis of 1-(4-vinylbenzyl)thymine and its polymerization by RAFT and ATRP techniques. *Polym. Preprints* **45,** 1061–1062 (2004).
37. Fukuda, T. *et al.* Mechanisms and kinetics of nitroxide-controlled free radical polymerization. *Macromolecules* **29,** 6393–6398 (1996).
38. Goto, A. & Fukuda, T. Kinetics of living radical polymerization. *Prog. Polym. Sci.* **29,** 329–385 (2004).
39. Kelley, E. G. *et al.* Structural changes in block copolymer micelles induced by cosolvent mixtures. *Soft Matter* **7,** 7094–7102 (2011).
40. Patterson, J. P. *et al.* A simple approach to characterizing block copolymer assemblies: graphene oxide supports for high contrast multi-technique imaging. *Soft Matter* **8,** 3322–3328 (2012).
41. Gons, J., Straatman, L. J. P. & Challa, G. Radical polymerization of methyl methacrylate in the presence of isotactic poly(methyl methacrylate). VIII. Influence of template concentration. *J. Polym. Sci. Polym. Chem. Ed.* **16,** 427–434 (1978).
42. Van de Grampel, H. T., Tan, Y. Y. & Challa, G. Template polymerization of *N*-vinylimidazole along poly(methacrylic acid) in water. 1. Influence of template concentration. *Macromolecules* **23,** 5209–5216 (1990).
43. Van de Grampel, H. T., Tan, Y. Y. & Challa, G. Template polymerization of *N*-vinylimidazole along poly(methacrylic acid) in water. 3. Molecular weights of the formed polymers. *Macromolecules* **24,** 3773–3778 (1991).
44. Ganeva, D. E. *et al.* Particle formation in *ab initio* RAFT mediated emulsion polymerization systems. *Macromolecules* **40,** 6181–6189 (2007).
45. Uemura, T., Ono, Y., Kitagawa, K. & Kitagawa, S. Radical polymerization of vinyl monomers in porous coordination polymers: nanochannel size effects on reactivity, molecular weight, and stereostructure. *Macromolecules* **41,** 87–94 (2008).
46. Serizawa, T., Hamada, K. & Akashi, M. Polymerization within a molecular-scale stereoregular template. *Nature* **429,** 52–55 (2004).
47. Percec, V., Ahn, C. H. & Barboiu, B. Self-encapsulation, acceleration and control in the radical polymerization of monodendritic monomers via self-assembly. *J. Am. Chem. Soc.* **119,** 12978–12979 (1997).
48. Percec, V. *et al.* Controlling polymer shape through the self-assembly of dendritic side-groups. *Nature* **391,** 161–164 (1998).
49. Rzayev, J. & Penelle, J. HP-RAFT: a free-radical polymerization technique for obtaining living polymers of ultrahigh molecular weights. *Angew. Chem. Int. Ed.* **43,** 1691–1694 (2004).
50. Percec, V. *et al.* Ultrafast synthesis of ultrahigh molar mass polymers by metal-catalyzed living radical polymerization of acrylates, methacrylates, and vinyl chloride mediated by SET at 25 °C. *J. Am. Chem. Soc.* **128,** 14156–14165 (2006).
51. Nicolaÿ, R., Kwak, Y. & Matyjaszewski, K. A green route to well-defined high-molecular-weight (co)polymers using ARGET ATRP with alkyl pseudohalides and copper catalysis. *Angew. Chem. Int. Ed.* **49,** 541–544 (2010).
52. Ouchi, M., Badi, N., Lutz, J-F. & Sawamoto, M. Single-chain technology using discrete synthetic macromolecules. *Nature Chem.* **3,** 917–924 (2011).

Acknowledgements

The authors thank the University of Warwick and the Engineering and Physical Sciences Research Council (grant reference: EP/H019146/1) for funding. The authors also acknowledge the Precision Polymer Materials Research Networking Programme of the European Science Foundation for funding. Some items of equipment used in this research were funded by Birmingham Science City, with support from Advantage West Midlands, and part funded by the European Regional Development Fund. We thank the Wellcome Trust (grant reference 055663/Z/98/Z) for the electron microscopy facility at Warwick. We thank O. Colombani, C. Chassenieux and T. Nicolai (all at Université du Maine, Le Mans, France) and A.H. Lu (University of Warwick) for assistance and advice on light-scattering experiments. We thank T. Wilks (University of Warwick) for assistance with graphic illustrations and C. Hansell (University of Warwick) for assistance with proof-reading. We would also like to thank M. Jewett (Northwestern University), P. Booth (University of Bristol) and A. Ellington (University of Texas, Austin) for insightful scientific discussions.

Author contributions

R.M. designed and performed the experiments and wrote the paper. J.P.P. performed the microscopy (TEM and AFM) and DSC, assisted with SLS and some synthesis and P.B.Z. designed the experiments. R.K.O.R. conceived and obtained funding for the project, designed the experiments, oversaw the research and finalized the manuscript. All authors discussed the results and commented on the manuscript.

Additional information

The authors declare no competing financial interests. Supplementary information accompanies this paper at www.nature.com/naturechemistry. Reprints and permission information is available online at http://www.nature.com/reprints. Correspondence and requests for materials should be addressed to R.K.O.R.